Field Performance of Aggregate-Lime-Pozzolan Base Material

M. C. Wang and W. P. Kilareski, Pennsylvania Transportation Institute, Pennsylvania State University, University Park

The behavior and performance of pavements that contain aggregate-lime-pozzolan (ALP) base are evaluated and compared with those of a pavement that contains a crushed-stone base. Performance data collected include present serviceability index, rut depth, and cracking. The response of the ALP pavement to 80-kN [18 000-lbf (18-kip)] equivalent axle loadings (EALs) is analyzed by using an elastic-layer computer program. Pavement response is related to performance data to establish limiting criteria. The limiting criteria developed constitute the basis for the determination of the structural coefficient of ALP material. The results of the study indicate that the ALP material, in comparison with the crushed-stone aggregate, provided a stiff base that considerably reduced rutting. Furthermore, the PSI value decreased much slower in the ALP pavement, and cracking developed much earlier and propagated much faster in the crushed-stone pavement. No non-traffic-associated cracking appeared in either type of pavement. The limiting criteria, which were developed for the ALP pavement to withstand 1 million EALs without significant surface cracking and excessive rutting, were a maximum pavement surface deflection of 0.28 mm (0.011 in), a maximum radial tensile strain at the bottom of the base course of 41.0 μm/m (0.000 041 in/in), and a maximum compressive strain at the top of the subgrade of 160.0 μm/m (0.000 160 in/in). Within the range of layer thicknesses studied, the structural coefficients of the ALP material were, approximately, 0.33, 0.29, and 0.25 for surface layer thicknesses of 3.8, 6.4, and 8.9 cm (1.5, 2.5, and 3.5 in), respectively.

There is ample evidence to indicate that lime with fly ash is an effective agent in stabilizing aggregate for pavement construction (1). The total energy required in the production of aggregate—lime—fly-ash (ALFA) mixes is very low because the mixes generally require a small amount of lime. On the other hand, the required fly-ash content is considerably high, usually from three to five times that of the required lime content. Thus, the use of fly ash for stabilization can at least alleviate the problem of disposing of the ever-increasing quantity of fly ash. These two factors have aided in the increasing use of ALFA material in recent years.

In spite of the increase in the use of ALFA material in pavement construction, most agencies base the thickness and quality design of ALFA layers on empirical rules. Although it is likely that some degree of empiricism will always be required to account for factors that are not readily analyzable, improved methods of thickness design are needed. General steps required for the development of an improved design technique have been proposed by the Committee on Structural Design of Roadways of the American Society of Civil Engineers (ASCE) (2). Included in these steps are the establishment of failure criteria and performance studies in the field.

A research program on the field performance of various base-course materials was undertaken at the Pennslyvania Transportation Research Facility of the Pennsylvania State University. The base-course materials studied were aggregate-lime-pozzolan (fly ash), dense-graded crushed stone, aggregate cement, bituminous concrete, and aggregate bituminous. The performance of aggregate cement and bituminous concrete pavements is discussed in papers by Wang and Larson and by Wang and Kilareski elsewhere in this Record. This paper discusses the performance of pavements that contain aggregate-lime-pozzolan base courses. Limiting strain criteria and limiting deflection criteria were developed from field performance data and data on pavement response. The results of this study provide information that would be useful in the design steps identified by ASCE.

AGGREGATE-LIME-POZZOLAN MATERIAL

The aggregate-lime-pozzolan (ALP) base material studied was composed of 3 percent by weight of lime, 15 percent by weight of fly ash, and 82 percent by weight of aggregate. The mix design was determined by the Bureau of Materials, Testing, and Research of the Pennsylvania Department of Transportation (PennDOT). The aggregate was a crushed limestone. The tables below summarize the gradation and the basic properties of the aggregate, lime, and fly ash (1 mm = 0.039 in):

Sieve Size (mm)	Percentage Passing: Aggregate	Lime	Fly Ash
50	100		
19	93		
9.5	53		
4.75	28		
2.36	17		
1.18	10		
0.6	7		
0.3	4		
0.15	2	97.7	94.7
0.075	-	85.4	82.7
0.045	-	82.9	68.8

Property	Percentage: Aggregate	Lime	Fly Ash
Specific gravity	2.78	-	2.40
Loss on ignition	-	16.0	-
Chemical composition			
SiO_2		Trace	45.3
Fe_2O_3		2.0	15.6
Al_2O_3			24.6
CaO		47.4	4.2
MgO		32.6	1.3
C		1.3	2.4

The chemical properties of lime and fly ash given in the second table are taken from the work of Cumberledge and others (3).

TEST PAVEMENTS

Four test pavements that contained ALP base were constructed at the Pennsylvania Transportation Research Facility. Two were installed in the summer of 1972, and the other two were constructed in the fall of 1975 (the construction of the base course took place from October 22 through November 3). Each of the four pavements contained a 6.4-cm (2.5-in) bituminous concrete surface and a 20.3-cm (8-in) subbase layer. The first two pavements had a 20.3-cm base; the other two pavements contained a 15.2-cm (6-in) and a 10.2-cm (4-in) base, respectively. One of the first two pavements was in a cut, and the other was in a fill section. The fill section was replaced by the last two pavements after about 1.1 million applications of 80-kN [18 000-lbf (18-kip)] equivalent axle loads (EALs) (EAL, as used in this paper, refers to an 80-kN load). Each of the first two pavements was 67.1 m (220 ft) long, and the length of each of the last two pavements was 30.5 m (100 ft). All pavements were 3.7 m (12 ft) wide.

The ALP material was mixed in a central plant at Talmage, Pennsylvania. The 10.2-cm (4-in) and 15.2-cm (6-in) ALP bases were placed in one lift, whereas the 20.3-cm (8-in) bases were placed in two 10.1-cm (4-in) compacted layers. The top of the first lift was scarified before placement of the second lift. Compaction was achieved by using a tandem-axle steel-wheel roller. After compaction, a bituminous seal coat was applied to the surface of the ALP base course. The moisture content and dry density were 6.7 percent and 2251 kg/m^3 (139.6 lb/ft^3), respectively, which corresponds to the optimum moisture content and maximum dry density of the modified American Association of State Highway and Transportation Officials (AASHTO) compaction effort.

In addition to the ALP pavements, the research facility also contained one pavement with a 20.3-cm (8-in) dense-graded, crushed-stone base and several other pavements with different base materials. The crushed-stone base had a 6.4-cm (2.5-in) bituminous concrete surface and a 20.3-cm subbase. This pavement was used to provide a comparative basis for the data obtained at the research facility with AASHO Road Test findings as well as with numerous other published findings on crushed-stone base courses. The design data for the crushed-stone base material are given below. The materials used were bituminous concrete fine aggregate and Pennsylvania 2B aggregate at a maximum dry density of 2327.7 kg/m^3 and an optimum moisture content of 7.5 percent. The field data represent an average of nine tests (1 mm = 0.039 in):

	Percentage Passing	
Sieve Size (mm)	Specification Limits	Field Data
50	100	100
19	52-100	85.0
9.5	36-70	55.1
4.75	24.50	41.2
2.36	-	32.2
1.18	10-30	21.3
0.6	-	14.8
0.3	-	10.9
0.15	-	8.8
0.075	0-10	-

The crushed-stone pavement was overlaid with 6.4 cm (2.5 in) of bituminous concrete after approximately 940 000 EAL applications.

The subgrade soil at the research facility was predominantly soil classification A-7. The first two ALP pavements (constructed in 1972) were subjected to traffic approximately two months after completion of the base-course construction. For the last two ALP and crushed-stone pavements (constructed in 1975), traffic was started about one month after the base course was completed. The traffic was initially provided by a conventional truck tractor that pulled a semitrailer and a full trailer. After about 1.5 million EALs, another full trailer was added to increase the rate of loading. The single-axle loading was within the range of 80-107 kN (18 000-24 000 lbf). Complete information on design, construction, material properties, and traffic operation is available elsewhere (4, 5).

FIELD EVALUATION

Field testing of pavement performance was conducted periodically. Rut depth was measured biweekly every 12.2 m (40 ft) in both wheel paths by using an A-frame that was attached to a 2.1-m (7-ft) long base channel. Surface cracking was surveyed and mapped biweekly. Surface roughness was measured in both wheel paths by using a MacBeth profilograph. The roughness factors obtained from the profilograph data were converted into pavement present serviceability index (PSI) by using Equations 1 and 2 given in the paper by Wang and Larson elsewhere in this Record.

Surface deflections were determined in the wheel paths by using the Benkelman beam and road-rater measurements. Pavement temperature profile and distribution of subgrade moisture were measured by using thermocouples and moisture cells. Two frost-depth indicators were installed at the research facility to measure the depth of frost penetration. Weather data such as wind velocity, precipitation, and temperature were collected by using various meteorological gages.

DISTRESS BEHAVIOR

The distress behavior of the test pavements was evaluated in terms of rutting and cracking. Figure 1 shows the rut-depth data for the ALP and crushed-stone pavements (the two short ALP pavements are not included since they did not cure properly because of cold weather during construction). The figure also shows the seasons in which the rut depths were measured. The two ALP pavements show almost the same amount of rutting until the point at which the fill section was replaced, which indicates that the material properties of the two pavements were quite consistent. Figure 1 clearly indicates that the ALP pavement has much greater resistance to rutting than the crushed-stone pavement. The rate of rutting seems to vary insignificantly with the seasons while the pavements are in structurally sound condition but to increase rapidly in the spring season when the pavements approach a state of failure.

Figure 1 shows that the crushed-stone pavement displayed rutting of about 25.4 mm (1.0 in) at the end of 1 million EAL applications, whereas the ALP pavement had only about 3.8-mm (0.15-in) rutting. The ALP pavement reached a rut depth of 6 mm (0.25 in) at about 1.4 million EALs, whereas the crushed-stone pavement reached this rut depth at only about 0.2 million EALs. The 6-mm rut depth is widely used as a criterion in the design of

Figure 1. Rut depth versus EAL for pavements with ALP and crushed-stone bases.

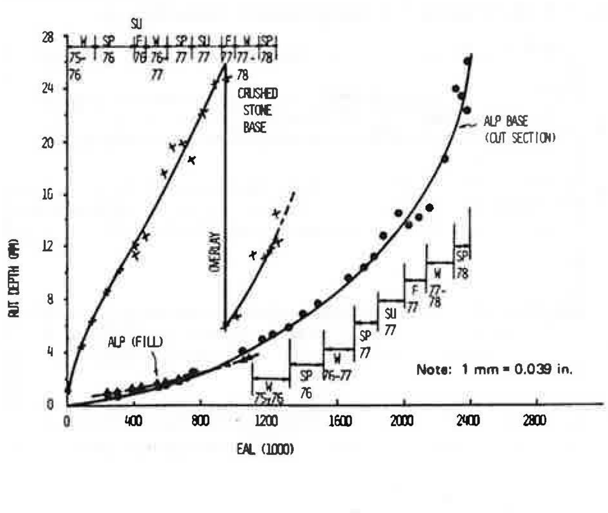

flexible highway pavements (6, 7). These data will be used later as a basis for the determination of the structural coefficient of the ALP material.

The results of a crack survey showed that there was no cracking in either 20.3-cm (8-in) ALP-base pavement at the time when the fill section was removed. A few hairline cracks appeared in the wheel paths in the cut section at approximately 1.12 million EAL applications. After about 2.3 million EALs, two potholes had formed in the ALP pavement. The first pothole developed at about 1.17 million EALs and the second at about 1.36 million EALs. Figures 2-5 show crack patterns mapped at four different times to illustrate the growth of surface cracking in the ALP pavement. It is interesting to note that nearly all cracks initiated in the longitudinal direction. The more numerous longitudinal cracks along the left side of the pavement were probably a result of the installation of a skid-testing facility adjacent to the left edge of the pavement. The construction of the skid-testing facility could have disturbed the original support along the edge of the test pavement. As a result, the edge of the test pavement is under less confinement and is thus more susceptible to the formation of longitudinal cracking.

Figure 2. Crack patterns in ALP pavement: April 1976.

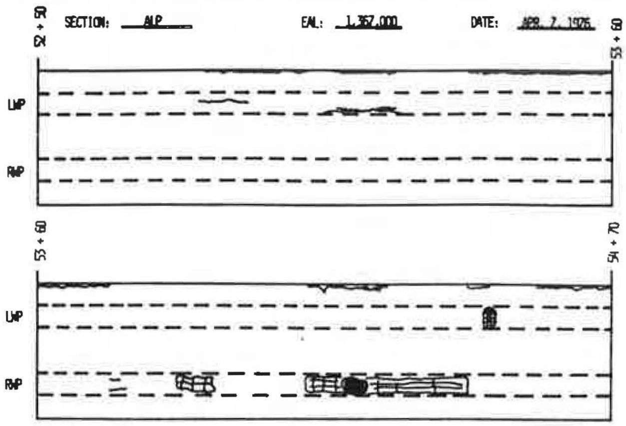

Figure 3. Crack patterns in ALP pavement: March 1977.

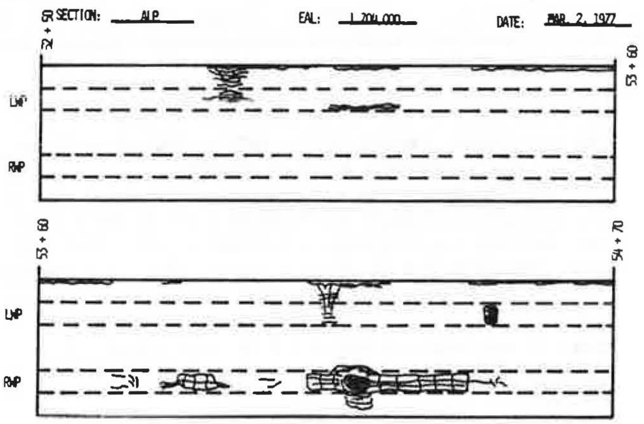

Figure 6 shows crack patterns developed in the crushed-stone pavement. Hairline cracks initiated in both wheel paths at approximately 56 500 EAL applications. The contrast in the development of surface crack patterns in the ALP and crushed-stone pavements is shown in Figures 2-6. In the ALP pavement, surface cracking initiated in some localized areas; in the crushed-stone pavement, surface cracking developed in the wheel paths at almost the same time throughout the entire pavement. One possible reason for the difference could be the nonuniformity of the ALP material, which is probably attributable to imperfect mixing. But no attempt was made to verify this. Figures 2-6 also show that the rate of growth from class 1 to class 2 and class 3 cracking was much faster in the crushed-stone pavement than in the ALP pavement. Furthermore, no apparent temperature or shrinkage cracking was observed in either pavement.

The total areas of class 2 and class 3 cracking that developed in both ALP and crushed-stone pavements are shown in Figure 7. The area of cracking increased very rapidly when the pavements approached a state of failure. A rapid increase in cracking occurred in the ALP pavement during the spring of 1976, primarily because of the development of the second pothole. During the spring season, the thawing of frozen material and relatively heavy rainfall contributed to the formation of potholes. It should be noted that, among the many test pavements at the research facility, potholes were observed only in the ALP pavement. Possible reasons for this are yet to be investigated.

PAVEMENT PERFORMANCE

The variation of PSI with EAL applications for the ALP and crushed-stone pavements is shown in Figure 8. The initial PSI values for the three pavements were almost the same, approximately 3.8. The performance trends of the two ALP pavements were also nearly equal until

Figure 4. Crack patterns in ALP pavement: November 1977.

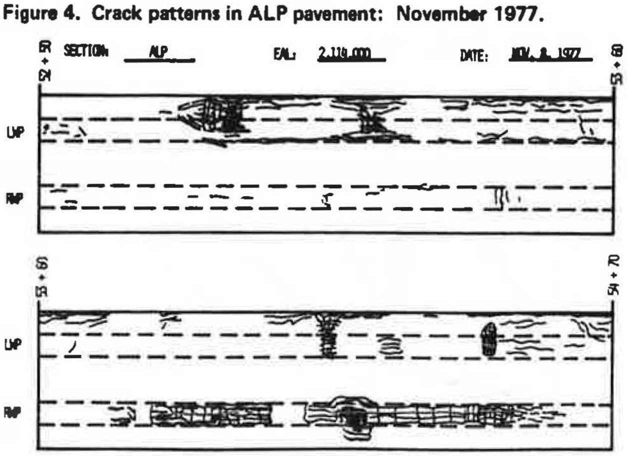

Figure 5. Crack patterns in ALP pavement: March 1978.

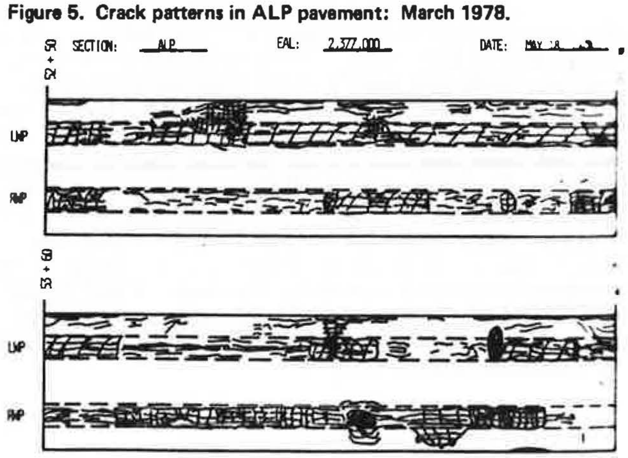

Figure 6. Crack patterns in crushed-stone pavement.

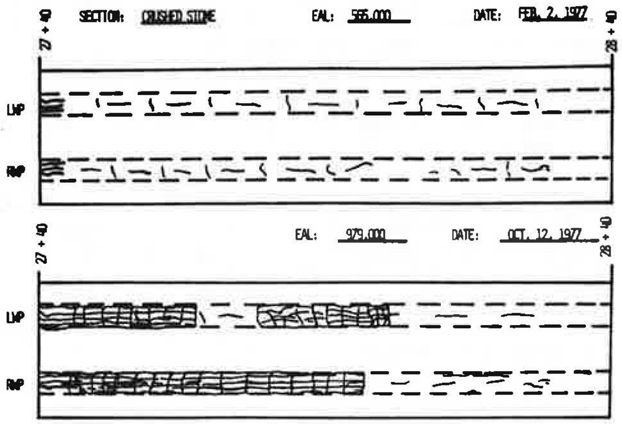

Figure 7. Crack area versus number of EALs.

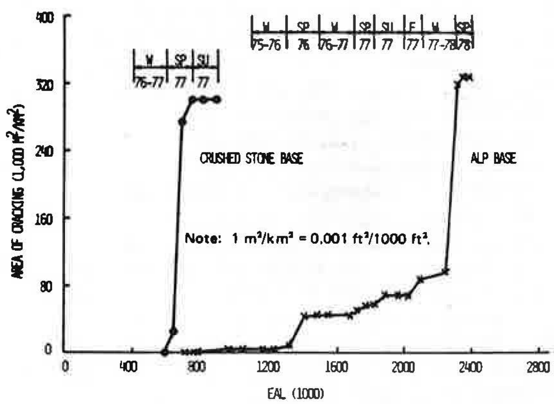

Figure 8. Variation of PSI with number of EALs.

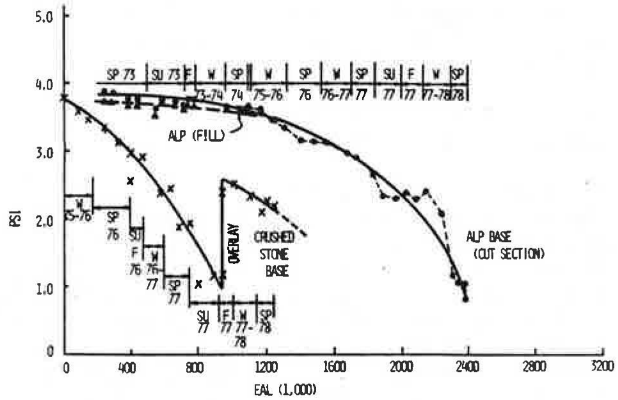

the fill section was removed. For the first million EAL applications, the PSI value decreased by only about 0.3. After that, however, the PSI value dropped at an ever-increasing rate. The data seem to show that the PSI dropped slightly faster in the spring-summer seasons than in the fall-winter seasons. According to the data, it required about 2.15 million EAL applications to reach a PSI of 2.0.

From the beginning, the PSI value dropped much faster for the crushed-stone pavement than for the ALP pavement, which would indicate a shorter service life for the crushed-stone pavement. The performance data also indicate that the crushed-stone pavement can only sustain 0.7 million EAL applications before it reaches a PSI of 2.0. This service life is much shorter than that of the ALP pavement. The PSI value immediately after overlay was only about 2.6, which is much lower than the PSI after initial construction. A possible reason for this could be that the crushed-stone pavement is so short—only 33 m (100 ft) long—that it is rather difficult to control the thickness of overlay uniformly by using routine construction equipment.

MATERIAL PROPERTIES

The strength and fatigue properties of the ALP material were determined based on specimens both compacted in the laboratory and taken from the pavement. The laboratory-compacted specimens were 15.2 cm (6 in) in diameter and 25.4 cm (10 in) in height and were molded by using the modified AASHTO compaction effort to the same moisture content and dry density as those in the pavement. The compacted specimens were embedded in the soil at the research facility to cure under the same environmental conditions as the test pavement. Several core samples 10.2 cm (4 in) in diameter and 20.4 cm (8 in) in height were taken from the test pavement after about 1.1 million EALs. Note that the 1.1 million EALs were achieved after approximately 20 months of traffic. Test results indicated that the laboratory-compacted specimens had almost the same strength properties as the core samples.

Triaxial compression tests were conducted on four-week-old and one-year-old specimens under various confining pressures up to 0.14 MPa (20 lbf/in²). Test results indicated no significant effect of confinement on the compressive strength within the range of conditions studied. Based on the results of six tests, average compressive strength and strain at failure were 17.1 MPa (2480 lbf/in²) and 0.0142, respectively, for one-year-old specimens and 5.2 MPa (750 lbf/in²) and 0.010, respectively, for four-week-old specimens.

The tensile strength of the test specimens was determined by using the double-punch test (8). For specimens aged 4 weeks, 10 weeks, 1 year, and 2 years, the tensile strengths were 0.24, 0.39, 0.84, and 0.97 MPa (34, 57, 121, 140 lbf/in²), respectively. By comparison with the previous values of compressive strength, the ratios of tensile to compressive strength are approximately 4.5 and 4.9 percent for 4-week-old and 1-year-old specimens, respectively. These two ratios are close to the lower limit of the range of values documented elsewhere (9).

The fatigue property was evaluated by using repeated-load flexural tests on beam specimens. The beam specimens, which were compacted in the laboratory, had dimensions of 8.25x8.25x45.75 cm (3.25x3.25x18 in). The beam specimens were simply supported at both ends and were subjected to repeated loading at two points within the span. Each loading point was located at equal distance from its nearest support to ensure pure bending at the middle of the span. The repeated loading had a duration of 0.1 s and a frequency of 20 cycles/min. Test results gave $K_1 = 2.80 \times 10^{-4}$ and $K_2 = 2.17$ for the following fatigue equation:

$$N = K_1 (1/\epsilon)^{K_2} \qquad (1)$$

where N = number of load repetitions to failure and ϵ = tensile strain.

In addition, repeated-load triaxial compression tests were conducted by using the same repeated loading to determine the modulus of resilient deformation. For confining pressures up to 0.21 MPa (30 lbf/in²) and deviatoric stresses up to 0.45 MPa (65 lbf/in^2), the resilient modulus was found to be practically independent of confining pressure, deviatoric stress, and the number of load repetitions. The resilient modulus was averaged at 16 400 MPa (2.38 million lbf/in^2).

PAVEMENT RESPONSE AND LIMITING CRITERIA

Pavement response was analyzed for the weather conditions that are most critical to pavement performance by using an elastic-layer computer program and the appropriate material properties. The computer program adopted was the BISAR program developed at Koninklijke Shell in Denmark. Material properties needed are the modulus of elasticity and Poisson's ratio of each pavement constituent material. The elastic modulus of the ALP material has already been given. Poisson's ratio is taken to be 0.15, according to previous research results (11).

The data on subgrade moisture indicated that the maximum subgrade moisture content occurred around the late spring and early summer. At this time of the year, the subgrade moisture content was approximately 21 percent and the average pavement temperature was about 21°C (70°F). The elastic moduli of the bituminous concrete surface, crushed-limestone subbase, and subgrade materials that correspond to these temperature and moisture conditions are 965.5 MPa (140 000 lbf/in^2), 330.9 MPa (48 000 lbf/in^2), and 68.9 MPa (10 000 lbf/in^2), respectively (10). In addition, Poisson's ratio values are 0.40, 0.40, and 0.45, respectively, for the surface, subbase, and subgrade materials. The critical response analyzed included maximum tensile strain in the surface and base courses, maximum vertical compressive strain in the subgrade, and maximum deflection on the pavement surface. These responses were considered because maximum tensile strain and maximum surface deflection are associated with fatigue cracking (11-14), whereas maximum vertical compressive strain is associated with rutting (6, 7, 13).

According to the results of the response analysis, maximum pavement surface deflection, maximum tensile strain at the bottom of the base course, and maximum subgrade compressive strain equal 0.27 mm (0.0107 in), 41.10 μm/m (0.000 041 in/in), and 142.78 μm/m (0.000 143 in/in), respectively. The field data presented earlier indicate that surface cracking appeared at approximately 1.1 million EAL applications. Thus, it would be appropriate to state that, for an ALP pavement to withstand 1 million EALs without surface cracking, the maximum pavement surface deflection and maximum tensile strain in the base course should be no greater than 0.28 mm (0.011 in) and 41.0 μm/m (0.000 041 in/in).

As mentioned before, the number of EAL repetitions required for 6 mm (0.25 in) of rutting is about 1.4 million (Figure 1). The maximum subgrade compressive strain obtained above is related to 1.4 million EAL repetitions in Figure 9. Figure 9 also shows the relations established for pavements with bituminous concrete bases at the research facility (10) and relations established by other researchers (6, 7, 13). It is estimated by extrapolation that the subgrade compressive strain at 1 million EALs equals approximately 160 μm/m (0.000 160 in/in). These three values—maximum surface deflection = 0.28 mm (0.011 in), maximum tensile strain = 41.0 μm/m (0.000 041 in/in), and maximum subgrade compressive strain = 160 μm/m (0.000 160 in/in)—constitute the limiting criteria for the ALP pavement to withstand 1 million EAL applications. One million EAL applications was adopted because it is widely associated with 20-year pavement service life.

Figure 9. Maximum compressive strain in subgrade versus EAL at 6-mm (0.25-in) rutting.

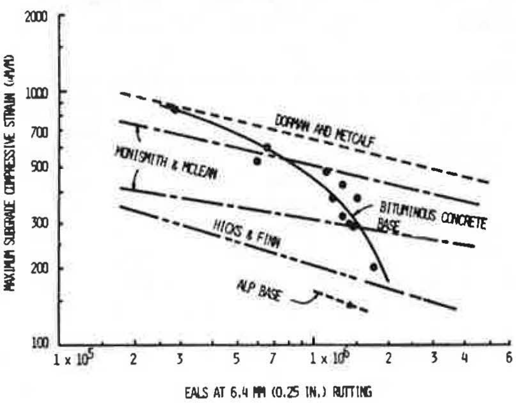

STRUCTURAL COEFFICIENT

The structural coefficient of the ALP base material was evaluated by following the same approach as that presented before (10). For this approach, the BISAR computer program was used to determine pavement sections that had various combinations of layer thickness that satisfied the preceding limiting criteria. Table 1 summarizes the results of the computation. The layer thicknesses in the first, second, and last columns of this table provide pavement sections for the calculation of the structural coefficient.

The structural coefficient was computed by using the

Table 1. Layer-thickness combinations that satisfy limiting criteria for ALP pavements.

Subbase Thickness (cm)	Surface Thickness (cm)	Base Thickness (cm) Based on: 0.028-cm Deflection	41.10-μm/m Tensile Strain	160.10-μm/m Compressive Strain	Combined
0	3.8	22.1	22.6	16.5	22.6
	6.4	21.3	19.6	15.7	21.3
	8.9	20.6	17.8	15.0	20.6
10.2	3.8	21.3	22.4	18.8	22.4
	6.4	20.8	21.3	18.3	21.3
	8.9	20.1	20.3	17.5	20.3
20.3	3.8	20.3	21.3	18.0	21.3
	6.4	19.6	20.3	17.5	20.3
	8.9	18.8	19.3	16.8	19.3
40.6	3.8	17.3	19.8	14.7	19.8
	6.4	16.5	18.8	14.2	18.8
	8.9	15.5	17.5	13.5	17.5

Note: 1 cm = 0.39 in; 1 μm/m = 0.000 001 in/in.

Figure 10. Structural coefficients of ALP and subbase materials.

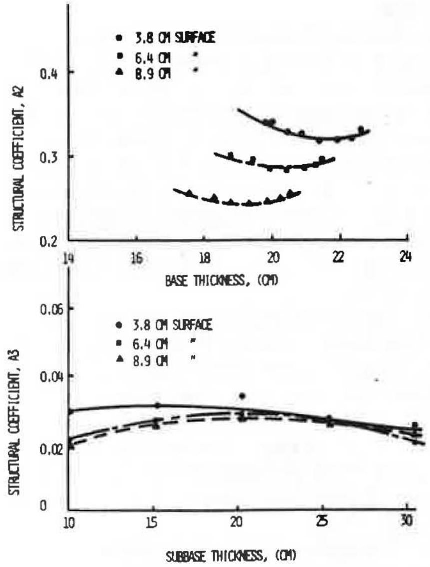

following basic equation, developed from the AASHO Road Test:

$$\rho = 0.64(SN + 1)^{9.36} \quad (2)$$

where ρ = EALs at failure and SN = structural number, which is defined as follows:

$$SN = a_1 H_1 + a_2 H_2 + a_3 H_3 \quad (3)$$

where a_1, a_2, and a_3 = structural coefficients of surface, base, and subbase materials, respectively, and H_1, H_2, and H_3 = layer thicknesses of surface, base, and subbase courses, respectively.

In the computation, a structural coefficient of 0.44, which was originally developed from the AASHO Road Test, was used for the bituminous concrete surface material. It was assumed that the structural coefficient of the subbase material does not change appreciably within a thickness of 5.1 cm (2 in). A more detailed computation procedure is available elsewhere (10). The structural coefficients determined are shown in Figure 10.

Figure 10 shows that, for a given surface-layer thickness, the structural coefficient of the ALP material is nearly constant within the range of base thicknesses studied. The structural coefficient of the ALP material, however, is smaller for thicker surface layers. The same effect was also observed for bituminous concrete base material (10). Figure 10 shows that the structural coefficients equal approximately 0.33, 0.29, and 0.25 for surface thicknesses of 3.8, 6.4, and 8.9 cm (1.5, 2.5, and 3.5 in), respectively. These values are close to those determined by Ahlberg and Barenberg (15) for other ALP materials; the values ranged between 0.34 and 0.20 for different qualities of ALP materials.

The structural coefficient of the limestone subbase material is also roughly independent of the subbase layer thickness, as shown in Figure 10. For the range of layer thicknesses studied, the average structural coefficient of the subbase material equals approximately 0.03. This value is relatively low compared with 0.10, the value that was reported before for bituminous concrete base material (10). This deviation could be attributed to the difference in relative stiffness between the base and subbase layers. As given earlier, the resilient modulus of the ALP material equals 16 400 MPa (2.38 million lbf/in^2) and that of the bituminous concrete base was approximately 2410 MPa (0.35 million lbf/in^2), which corresponds to the spring temperature condition (10). Thus, the relative stiffness between the ALP base and the subbase is considerably greater than that between the bituminous concrete base and the subbase materials. Since the combinations of layer thickness that satisfy the limiting criteria depend on the relative stiffness of the constituent layers, the effect on the base thickness of a unit change in the subbase thickness is less significant for the system that contains a base course much stiffer than the subbase course. As a consequence, the structural coefficient of the subbase material evaluated with the ALP base was lower than that of the subbase material evaluated with the bituminous concrete base. A similar effect of one layer's stiffness on another layer's structural coefficient has also been observed by VanTil and others (16).

SUMMARY AND CONCLUSIONS

The behavior and performance of pavements that contained ALP base were evaluated and compared with those of pavement that contained crushed-stone base. The critical response of the ALP pavement was analyzed by using the BISAR computer program and appropriate material properties. The response analyzed was related to performance data to establish limiting criteria. The structural coefficient of the ALP material was evaluated based on the limiting criteria developed.

The results of this study indicate that ALP material provides a stiffer base with longer service life than crushed-stone aggregate. The ALP pavement displayed much less severe rutting than the crushed-stone pavement. In addition, the PSI value decreased at a much lower rate for ALP pavement than for crushed-stone pavement. Cracking developed much earlier and faster in the crushed-stone pavement. No apparent non-traffic-associated cracking was observed in either type of pavement.

For the ALP pavement to withstand 1 million applications of 80-kN EAL, the maximum surface deflection, maximum tensile strain in the base, and maximum vertical compressive strain in the subgrade must be limited to 0.28 mm (0.011 in), 41 μm/m (0.000 041 in/in), and 160 μm/m (0.000 160 in/in), respectively. The structural coefficient of the ALP material remains relatively constant with respect to the base thickness but varies with the surface thickness. For surface thicknesses of 3.8, 6.4, and 8.9 cm (1.5, 2.5, and 3.5 in), the structural coefficients equal 0.33, 0.29, and 0.25, respectively.

ACKNOWLEDGMENT

The study presented here is part of a research project sponsored by the Pennsylvania Department of Transportation in cooperation with the Federal Highway Administration, U.S. Department of Transportation. Their support is gratefully acknowledged. We wish to express our gratitude to the National Crushed Stone Association for lending us its repeated-load test apparatus for laboratory testing. Our sincere appreciation is extended to T. D. Larson of the Pennsylvania Transportation Institute for his encouragement and review of the manuscript. We are also thankful to S. A. Kutz for his participation in the preparation of the paper. The field data reported here were collected and reduced with the assistance of R. P. Anderson, B. A. Anani, P. J. Kersavage, and S. A. Kutz.

This paper represents our views and does not necessarily reflect those of the Pennsylvania Department of Transportation or the Federal Highway Administration.

REFERENCES

1. State of the Art: Lime Stabilization Reactions, Properties, Design, Construction. TRB, Circular 180, Sept. 1976.
2. Problems of Designing Roadway Structures. Transportation Engineering Journal, Proc., ASCE, Vol. 95, No. TE2, May 1969, pp. 289-315.
3. G. Cumberledge, G. L. Hoffman, and A. C. Bhajandas. Curing and Tensile Strength Characteristics of Aggregate-Lime-Pozzolan. TRB, Transportation Research Record 560, 1976, pp. 21-30.
4. E. S. Lindow, W. P. Kilareski, G. O. Bass, and T. D. Larson. An Evaluation of Pennsylvania's Flexible Pavement Design Methodology: Volume 2—Construction, Instrumentation, and Operation. Pennsylvania Transportation Institute, Pennsylvania State Univ., University Park, Interim Rept. PTI 7504, Feb. 1973.
5. W. P. Kilareski, S. A. Kutz, and G. Cumberledge. A Study of Flexible Pavement Base Course and Overlay Designs: Modification, Construction, and Instrumentation of an Experimental Highway. Pennsylvania Transportation Institute, Pennsylvania State Univ., University Park, Interim Rept. PTI 7607, April 1976.
6. G. M. Dormon and T. Metcalf. Design Curves for Flexible Pavements Based on Layered System Theory. HRB, Highway Research Record 129, 1966, pp. 60-75.
7. C. L. Monismith and D. B. McLean. Structural Design Considerations. Proc., AAPT, Vol. 41, 1972, pp. 258-305.
8. W. F. Chen. Double-Punch Test for Tensile Strength of Concrete. ACI Journal, Vol. 67, Dec. 1970, pp. 993-995.
9. Lime-Fly Ash-Stabilized Bases and Subbases. NCHRP, Synthesis of Highway Practice 37, 1976.
10. M. C. Wang and T. D. Larson. Performance Evaluation for Bituminous-Concrete Pavements at the Pennsylvania State Test Track. TRB, Transportation Research Record 632, 1977, pp. 21-27.
11. C. L. Monismith, J. A. Epps, D. A. Kasianchuk, and D. B. McLean. Asphalt Mixture Behavior in Repeated Flexure. Institute of Transportation and Traffic Engineering, Univ. of California, Berkeley, Rept. TE70-5, 1970.
12. R. I. Kingham. Fatigue Criteria Developed from AASHO Road Test Data. Proc., 3rd International Conference on the Structural Design of Asphalt Pavements, Univ. of Michigan, Ann Arbor, 1972, pp. 656-660.
13. R. G. Hicks and F. N. Finn. Prediction of Pavement Performance from Calculated Stresses and Strains at the San Diego Test Road. Proc., AAPT, Vol. 43, 1974, pp. 1-40.
14. E. Zube and R. Forsyth. Flexible Pavement Maintenance Requirements as Determined by De[illegible] Measurements. HRB, Highway Research R[illegible] 129, 1966, pp. 60-75.
15. H. L. Ahlberg and E. J. Barenberg. Poz[illegible] Pavements. Engineering Experiment Stat[illegible] of Illinois, Urbana-Champaign, Bull. 473, [illegible]
16. C. J. VanTil, B. F. McCullough, B. A. V[illegible] and R. G. Hicks. Evaluation of AASHO Int[illegible] Guides for Design of Pavement Structures. NCHRP Rept. 128, 1972.

Publication of this paper sponsored by Committee on Flexible Pavement Design.

Structural Design of PCC Shoulders

Jihad S. Sawan and Michael I. Darter, Department of Civil Engineering, University of Illinois, Urbana-Champaign

A structural design procedure for plain jointed portland cement concrete (PCC) highway shoulders has been developed. The procedure can be used to provide PCC shoulders either for rehabilitation of existing pavement or for new pavement construction. All major factors that are known to affect the behavior of PCC shoulders are considered in the mechanistic design approach, including encroaching moving trucks, parked trucks, foundation support, load transfer across the longitudinal joint, shoulder slab thickness and tapering, width of shoulder, and traffic lane slab. The finite-element structural analysis technique was used along with a model for concrete fatigue damage to sum damage for both moving encroaching trucks and parked trucks. A relation was established between accumulated fatigue damage and slab cracking. The shoulder can thus be designed for an allowable amount of cracking, which can vary depending on the performance level desired. Procedures for tying the PCC shoulder to the mainline PCC slab are recommended to provide adequate load transfer and avoid joint spalling. Long-term, low-maintenance performance of the PCC shoulder, as well as significant improvement in the performance of the traffic lane, can be obtained if the shoulder is properly designed.

Portland cement concrete (PCC) shoulders have been constructed for several years on urban expressways and rural highways. They were first constructed on an experimental basis but more recently as regular construction. Since no structural design procedure is available, design has been based on engineering judgement and the performance of a few experimental sections. The purpose of this study is to develop a structural design procedure that considers the major design variables that affect the behavior of PCC shoulders. The design includes the placement of PCC shoulders for the purpose of rehabilitating existing pavements and also for new pavement construction.

Shoulders are an integral part of today's major highways and are required to provide structural support to (a) encroaching traffic loads from the adjacent traffic lane, (b) emergency parking, and (c) regular traffic if the shoulder is used as a detour around a closed lane or as an additional lane during peak traffic hours. Field results of this study (1) have shown that the PCC shoulder contributes to the structural support of traffic in the adjacent lane so that distress in the lane is significantly